REGULAR ARTICLE

Oxidation states, atomic charges and orbital populations in transition metal complexes

Gabriel Aullón · Santiago Alvarez

Abstract The differences and similarities between calculated atomic charge and formal oxidation state in transition metal complexes are discussed in the light of density functional theory calculations on a variety of four-coordinate complexes. It is shown that the oxidation state formalism provides a framework for the classification of families of compounds related by ligand substitution or redox processes, and can neither be replaced by nor deduced from net atomic charges.

Keywords Transition metals · Oxidation states · Population analysis · DFT calculations · Pauling electroneutrality rule

1 Introduction

Transition metal complexes may undergo redox processes through which they adopt different charge states. It is customary to ascribe the addition or loss of one electron in such processes to the transition metal atom, except for those systems with non-innocent ligands that may be involved in ligand-centered electron transfer reactions. As a result, we assign an oxidation state to the metal atom and a corresponding d^n electron configuration. Both become important pieces of information to identify a given compound. In addition to the redox behavior, properties such as magnetism, color and stereochemistry are strongly dependent on the oxidation state and number of valence electrons.

The astonishing variety of oxidation states that transition metals can adopt (Fig. 1) is in part responsible for their rich chemistry. The available oxidation states cover all the range from clearly negative (-4) to highly positive ($+8$). Notice also that up to 11 different oxidation states are known for several metals (Cr, Mo, W, Mn, Re, Ru and Os).

In general, however, the accessibility of low and high oxidation states depends on the nature of the ligands. Thus, examples of transition metals in their lowest oxidation states invariably correspond to complexes with ligands that occupy the highest positions in the spectrochemical series, such as CO and PPh_3 (Fig. 2). In contrast, the highest oxidation state is only attained in the presence of highly electronegative donor atoms such as oxygen or fluorine. Such a behavior can be rationalized within the framework of the hard and soft acids and bases model (HSAB) [3], since a metal becomes a harder Lewis acid as its oxidation state is increased, and is therefore expected to form more stable compounds with hard Lewis bases such as the fluoride and oxide ions. Conversely, metals in low oxidation states are softer acids and form more stable compounds with soft bases such as carbon monoxide or phosphines.

With the advent of faster computers and more efficient software packages, computational studies of transition metal compounds have become a common complement to experimental research, especially given the relatively low computational cost of density functional theory (DFT) calculations. From those calculations it is easy to extract atomic charges obtained through one of several available

G. Aullón · S. Alvarez (✉)
Departament de Química Inorgànica, Institut de Química Teòrica i Computacional (IQTC), Universitat de Barcelona, Martí i Franquès 1-11, 08028 Barcelona, Spain
e-mail: santiago@qi.ub.es

Fig. 1 Minimum (*lower left corner*) and maximum (*upper right corner*) oxidation states known for each transition metal, expanded and updated by the authors from [1, 2]

Fig. 2 Examples of known compounds with a transition metal in its highest and lowest oxidation states, expanded and updated from [1]

population analysis schemes, and one is tempted to try to correlate the calculated charge at a metal atom with its oxidation state. In particular, we were prompted to investigate on the relationship between atomic charge and oxidation state by a recent debate on chemical bonding held by Roald Hoffmann, Carlo Mealli and one of the authors [4]. One of the points raised in that debate was an early proposal of Snyder [5–7], based on a population analysis, that the copper atom in $[Cu(CF_3)_4]^-$ should be assigned a Cu^I oxidation state rather than the commonly accepted Cu^{III}.

To provide a wider perspective of the trends in the calculated charges at the metal atom in coordination complexes, and of their relationships with formal oxidation states, we present here the results of DFT calculations for a variety of simple complexes. In particular, we will discuss the effects of the metal oxidation state and of the electronegativity of the donor atoms on the calculated metal charges. We will show that the relationship between formal oxidation state of the metal and its calculated atomic charge is not straightforward, and that there is a wide range of variability of the charge for a metal in complexes with the same oxidation state but different ligands.

2 Oxidation states and atomic charges

Let us start by asking ourselves: how do we assign an oxidation state to an atom M in an $[MX_m]^{n-}$ complex? What we do is to define a Lewis structure and assign the

electron pair associated to each M–X bond either in a covalent way (one electron to each participant in the bond (**2**), or in one of two ionic forms, depending on whether we consider M to be a Lewis acid and X a Lewis base (**1**), or viceversa (**3**), based on electronegativity criteria. Once the electrons are assigned, we count the number of valence electrons at each atom and obtain their oxidation states.[1]

$$M \longleftarrow : X \qquad M \bullet \bullet X \qquad M : \longrightarrow X$$

$$\textbf{1} \qquad\qquad \textbf{2} \qquad\qquad \textbf{3}$$
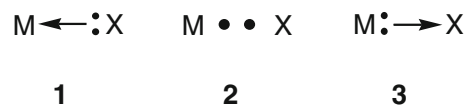
When M is a transition metal in an $[MX_m]^{n-}$ complex with X being, e.g., a halogen, we usually adopt the ionic extreme **1**, the m bonding electrons pairs are assigned to the anionic ligands X^- and the metal atom is left with an $(m - n)$ formal charge. In the purely covalent situation **2**, we ascribe m bonding electrons to the metal (one per each M–X bond) and one to each ligand, giving a formal charge of $-n$ at the metal. Finally, complete electron donation from the metal to the ligand **3** would imply the assignment of all eight bonding electrons to the metal, which would then have a formal charge approaching $-(m + n)$.

Although the limiting charges expected for the extreme models **1**–**3** cover a range of eight units for $[CuX_4]^{n-}$ ($n = 1$–3), the computational results show much less variability than the formal oxidation states. This is exemplified by $[Cu(CF_3)_4]^{n-}$ and other complexes with donor atoms of low electronegativity, in which the copper charge gives values intermediate between those expected for the ionic and covalent models **1** and **2** (Fig. 3), and varies little with the oxidation state. It is worth noting that the calculated charge becomes closer to that of the ionic model as the oxidation state of the metal decreases. Using a strongly electronegative ligand such as He results in a larger variability of the calculated charges with the oxidation state, with values much closer to the ionic limit **1**, while complexes with N or F donor atoms present an intermediate behavior.

The little dependence of the atomic charge on the oxidation state can be rationalized according to an early proposal by Pauling, who made a distinction between oxidation state and actual charge. Based on the electrostatic principle that an electrically charged solid metal sphere has its charge entirely on its surface, he proposed the *electroneutrality rule* [8, 9], which states that "the electronic structure of substances is such as to cause each atom to have essentially zero resultant electrical charge, the amount

---

[1] In Pauling's words: "In a covalent compound of known structure, the oxidation number of each atom is the charge remaining on the atom when each shared electron pair is assigned completely to the more electronegative of the two atoms sharing it" [8].
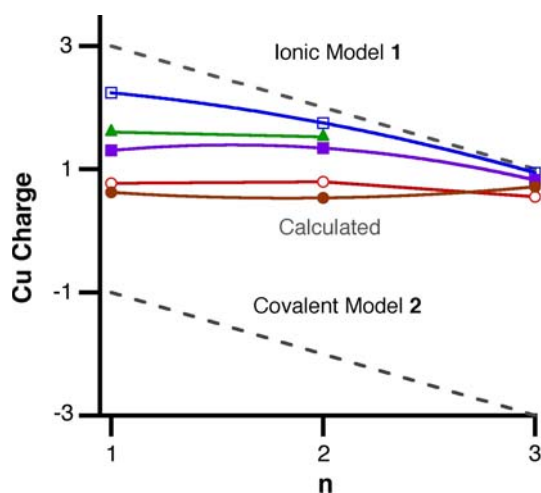
Fig. 3 Limiting values of the charge at the Cu atom according to the Lewis structures **1** and **2** (*dashed lines*), and calculated values for the following complexes: $[CuHe_4]^{4-n}$ (open squares), $[CuF_4]^{n-}$ (*triangles*), $[Cu(NH_3)_4]^{4-n}$ (filled squares), $[Cu(CF_3)_4]^{n-}$ (empty circles), and $[Cu(PH_3)_4]^{4-n}$ (filled circles). The values for $[CuH_4]^{n-}$, $[Cu(AsH_3)_4]^{4-n}$ and $[Cu(SbH_3)_4]^{4-n}$ (not shown) are practically coincident with the lowest curves

of leeway being not greater than about ±½". Remarkably, the computed copper charges shown in Fig. 3 present values between +0.5 and +0.8 in the presence of donor atoms of low electronegativity, such as H, As, P, Sb, Si or Sn, but the most electronegative donor atoms, F and He, give significantly higher charges that approach the value of the formal oxidation state.

3 Electronegativity of donor atoms and atomic charges

We have seen above that changes in the oxidation state of the metal atom bring about variations in the ionic/covalent character of the metal–ligand bonding. Alternatively, we may tune the covalency by changing the electronegativity of the donor atoms while keeping the oxidation state constant, as could be done by ligand substitution reactions, real or fictitious. It is well known, for instance, that a metal with a given oxidation state may have quite different redox potentials depending on the ligands coordinated to it [10]. Thus, the Lever parameter E_L [11] that calibrates the contribution of just one ligand to the electrode potential of a complex, has values ranging from −0.59 to +0.99 V. This translates to differences of about 15 kJ/mol in the free energy of the corresponding redox reactions, indicative of significant changes in localization/delocalization and energy of the HOMO and LUMO, typically with a dominant metal d character. If we change all the ligands in a six-coordinate complex, for instance, dramatic changes in the electrode potential may result for the same metal and

oxidation state, as found when comparing $[Fe(CN)_6]^{4-}$ and $[Fe(NCMe)_6]^{2+}$, with E^0 values of −0.31 and 2.64 V, respectively [10].

Our calculations for several Cu complexes show (Fig. 4) that, for a given oxidation state, the calculated charge at the copper atom increases with increasing electronegativity of the donor atoms. Such a trend nicely reflects an increasing ionic character of the metal–ligand bonds with more electronegative donors, because the calculated charge approaches the formal oxidation state as the donor becomes more electronegative. However, the charge in the Cu^{III} complexes does not reach the limit of the ionic model (i.e., its +3 formal oxidation state) even with the most electronegative ligands. As we move to lower oxidation states of the metal, the atomic charges with the most electronegative ligands become closer and closer to the formal oxidation state, giving a charge of +0.94 in the Cu^I complex $[CuHe_4]^+$. It is also remarkable that the Cu atomic charges do not significantly change with the oxidation state when less electronegative donors are present. Another interesting result is that with the most electropositive donor atoms tried (Sn, Si and Sb), the copper charge is still significantly higher (+0.5 and −0.5 with the NPA and APT population analysis, respectively) than the value expected for a covalent model **2** (−1.0), even if their electronegativities are nearly identical to that of copper (1.72 in the Allred-Rochow scale).

All the information presented in Fig. 4 can be translated to the language of chemistry in a schematic way (Fig. 5), in which all complexes with the same oxidation state are represented by a line with different slope. We can move
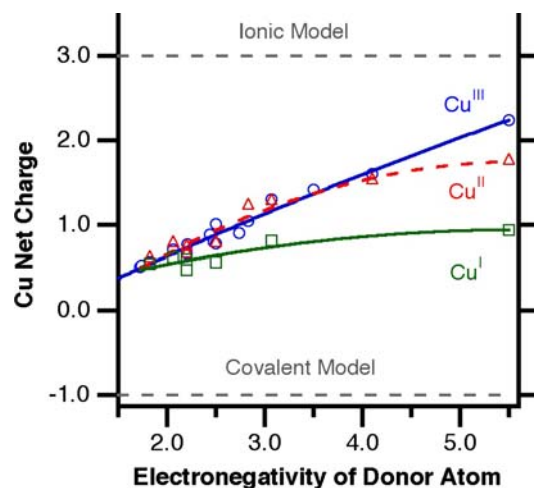
Fig. 4 Calculated charges at the Cu^{III} ion in $[CuX_4]^-$ (X = CH_3, CF_3, SiH_3, SnH_3, H, F, Cl, Br, I, OH, SH and SeH) and $[CuL_4]^{3+}$ (L = NH_3, PH_3, AsH_3, SbH_3 and He) complexes (*circles*), compared to the formal charges corresponding to the ionic (**1**) and covalent (**2**) Lewis structures. The values for some analogous Cu^{II} and Cu^I complexes are represented by *triangles* and *squares*, respectively
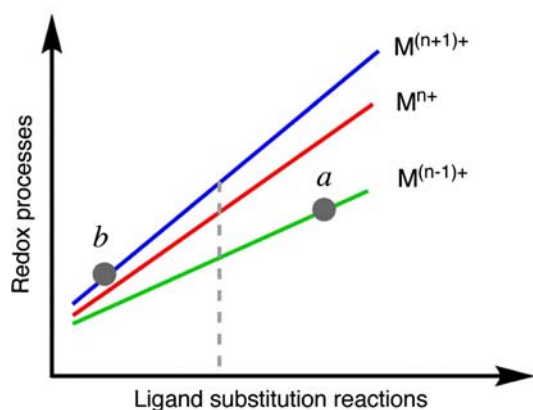
Fig. 5 Schematic representation of Fig. 4 showing the chemical relationships among complexes of the same metal and formal oxidation state (*continuous lines*), and with the same ligand but different oxidation states (*dashed line*)


Fig. 6 Calculated copper–ligand bond distances in several homoleptic complexes as a function of the Cu oxidation state, and experimental Cu–C distances (*open squares*)

along each of those lines, at least formally, through ligand substitution reactions, in which the oxidation state remains constant. Conversely, we can move vertically, from one oxidation state to another one by redox processes in which the coordinated ligands remain the same. In the case of the copper complexes studied here, all those with the same oxidation state (the same line in Fig. 5) have the same stereochemistry: tetrahedral for Cu^{I}, flattened tetrahedral for Cu^{II} and square planar for Cu^{III}.

Paradoxically, a given compound with a low oxidation state and a highly electronegative ligand (e.g., point *a* in Fig. 5) may have a higher charge at the metal atom than another complex with a higher oxidation state and a less electronegative ligand (e.g., point *b* in Fig. 5). This is why we use the term *formal oxidation state* to emphasize the lack of a direct correlation between this parameter and the atomic charge that we may obtain from DFT or post-Hartree-Fock calculations through some population analysis scheme. Despite the lack of quantitative physical meaning of the oxidation state, it is full of chemical significance, providing us with a framework for classifying a variety of compounds, and for describing the vertical (redox) and diagonal (ligand substitution) relationships among them.

4 Oxidation state, stereochemistry and bond distances

As expected for metal ions with d^8, d^9 and d^{10} electron configurations [12], the optimized geometries of the $[CuX_4]^{n-}$ anions are square planar, flattened tetrahedral and perfectly tetrahedral (for $n = 1$, 2 and 3, respectively), according to the corresponding continuous shape measures [13]. The same stereochemical behavior is found for the complexes with neutral ligands $[CuL_4]^{4-n}$. Also the copper–ligand bond distances show a dependence on the
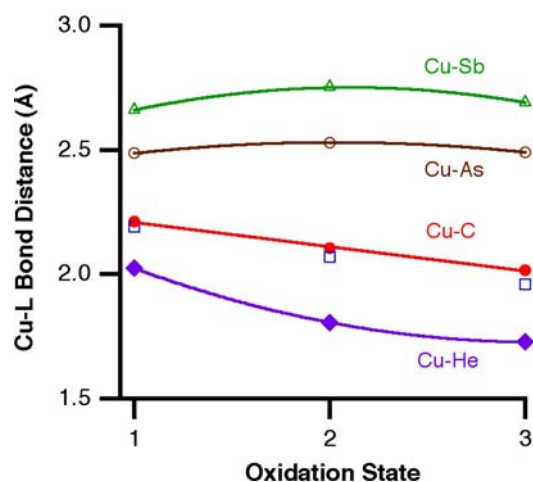
oxidation state for the less covalent complexes (Fig. 6), which could be attributed to increased electrostatic attraction between metal and ligand or to the enhanced covalent character of that bond. In the case of the Cu–C bonds, the calculated distances are just slightly longer than the corresponding experimental values in copper(I) [the mean value for seven organometallic Cu(I) compounds found in the Cambridge Structural Database is 2.19 (10) Å], (II) [14] and (III) [15–17] complexes, as usually found in B3LYP calculations, but the dependence on the oxidation state is remarkably similar to the experimental one.

5 Zooming in on the metal atomic orbitals

We focus now on the metal atomic orbitals that participate in metal–ligand bonding in the square planar complexes (x^2–y^2, $4s$, $4p_x$ and $4p_y$), whose acceptor ability toward the ligands are expected to be different, given their different energies and overlap with the ligand orbitals. For the family of Cu^{III} complexes, $[CuX_4]^-$ and $[CuL_4]^{3+}$, the population of the copper atomic orbital varies with the electronegativity of the donor atom as shown in Fig. 7. The population of the x^2–y^2 orbital increases with decreasing electronegativity of the donor atom. Even with the more electropositive donor atom studied (Sn), the population of the acceptor x^2–y^2 orbital is significantly smaller than 2 (1.81), to be compared with occupations of 1.99–2.00 electrons for the rest of the d orbitals in all compounds analyzed, with the exception of the He compound (average occupation of 1.97 electrons). Extrapolation of the trend observed in Fig. 7 tells us that only for donor atoms with an Allred-Rochow electronegativity of ~1.0 would x^2–y^2
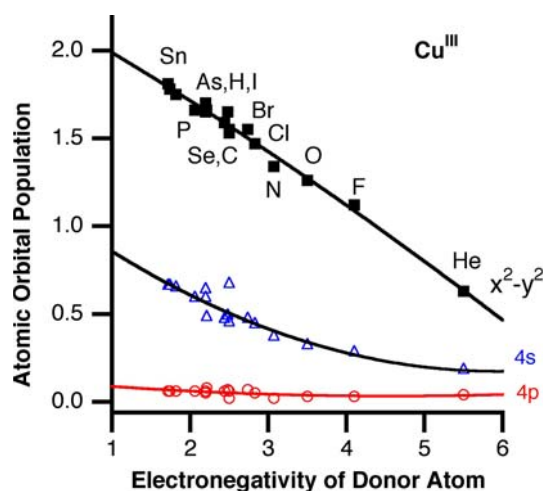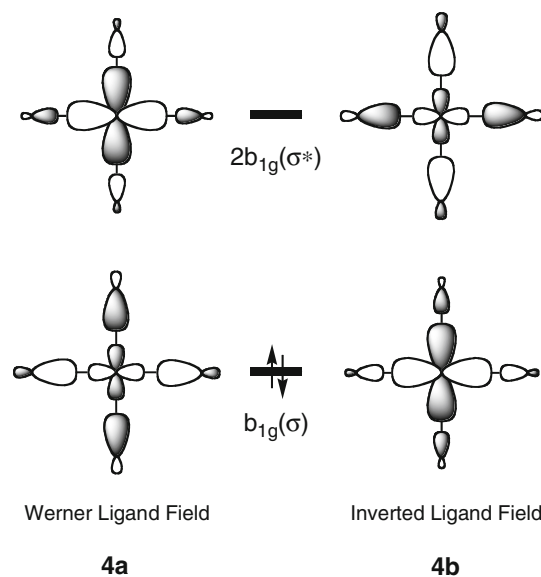
Fig. 7 Calculated population of the Cu atomic orbitals in $[CuX_4]^-$ (X = CH_3, CF_3, SiH_3, SnH_3, H, F, Cl, Br, I, OH, SH and SeH) and $[CuL_4]^{3+}$ (L = NH_3, PH_3, AsH_3, SbH_3 and He) complexes, as a function of the electronegativity of the donor atom. The *labels* indicate the donor atom for most points in the *upper curve*

become full. That value corresponds to the alkaline or alkaline-earth elements.

Except for the most electronegative ligands, the high population of the x^2-y^2 atomic orbital indicates that it has a higher participation in the occupied bonding b_{1g} MO than the ligand lone pair orbitals (**4b**), opposed to the common behavior of Werner-type complexes (**4a**). According to Hoffmann, the implications of this bonding situation—that he calls *inverted ligand field* (R. Hoffmann, personal communication, September 4, 2008)—has been poorly investigated and deserves further research.[2] Notice, however, that the degree of localization of the b_{1g} MO at the metal atom shows a marked continuous variation with changing ligands (i.e., a diagonal displacement in Fig. 5). In contrast, a change in the formal oxidation state from Cu^{III} to Cu^{II} (a vertical displacement in Fig. 5) does not significantly affect the population of x^2-y^2 in the complexes with less electronegative ligands (CF_3^- and H^-), and varies as little as 0.1 electron for such an electronegative ligand as fluoride. It must be noted, though, that the population in the two oxidation states has different meanings. While in the Cu^{II} complexes a good portion of the x^2-y^2 population has positive spin, the Cu^{III} analogs have only paired spin population. Interestingly, the α population in the case of Cu^{II} is in all cases of 1.0, and it is the β
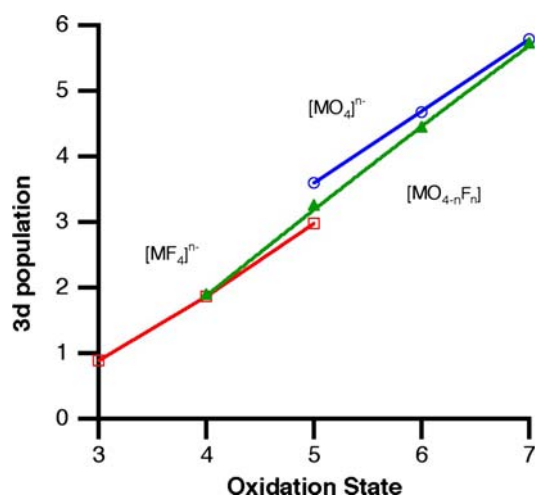
population that significantly varies with the electronegativity of the donor atoms.

The population of the copper $4s$ orbital also increases monotonically as the electronegativity of the donor atom decreases, in keeping with an enhanced covalent character of the copper–ligand bonds. The population of the copper $4p$ orbitals, in contrast, is very small and shows no significant changes with the ligand's electronegativity. The differences in the degree of occupation of the different Cu atomic orbitals involved in metal–ligand bonding, and in their susceptibility to the electronegativity of the ligand, nicely reflect the inverse dependence of their mixing coefficients on the reciprocal of the orbital energy difference, according to perturbation theory [19].

6 The case of the d^0 ions

The behavior of the ubiquitous tetrahedral oxoanions of d^0 metals in regard with the occupation of their d orbitals is remarkable. Consider the series formed by the vanadate, chromate and permanganate anions, $[VO_4]^{3-}$, $[CrO_4]^{2-}$ and $[MnO_4]^-$. Even if the oxidation states are +5, +6 and +7, the calculated metal charges are very similar for all of them (1.05, 1.09 and 0.96, respectively). Similarly, for the fluoro complexes $[ScF_4]^-$ and $[TiF_4]$, the net charge at the metal is the same (1.97), significantly higher than in the oxo complexes, even if the oxidation states are lower. Apparently, it is the electronegativity of the ligands that affects most the net charge at the metal atom, irrespective of its oxidation state. This means that for complexes with the same ligands, increasing oxidation states are compensated by an enhanced donation of electron density from the

---

[2] A significant example of an inverted ligand field was found in band electronic structure calculations of the $LaFe_4P_{12}$ skutterudite, which showed that the Fermi level has more phosphorus than Fe $3d$ character, and lead to the conclusion that its superconductivity is associated with the phosphorus sublattice rather than with the iron atoms [18].

Fig. 8 Calculated population of the 3d orbitals in the families of d^0 oxo-, fluoro- and oxyfluoro complexes with different oxidation states

ligands, resulting in higher population of the d orbitals (Fig. 8). These computational results provide a nice illustration of the Pauling electronegativity rule discussed above.

Another interesting observation is that the 3d orbital populations of the d^0 [MnO$_4$]$^-$ and the d^5 [FeF$_4$]$^-$ anions are practically identical (5.8). While one might feel comfortable with that value for the d^5 ion, it seems pretty high for the d^0 configuration. But the latter clearly does not correspond to a d^5 configuration, which would imply occupation of all 3d orbitals with one unpaired electron and, therefore, a net 3d spin density close to 5.0 (our calculations give a spin density of 4.17 for [MnO$_4$]$^-$, resulting from 4.99 α and 0.82 β electrons). On the contrary, the large electron density at the 3d orbitals in the d^0 ion corresponds fully to paired spins and a null spin density at the metal atom, resulting from partial donation of the ligand lone pairs.

7 Conclusions

The net charge calculated at the metal atom is, in most of the complexes studied, closer to the formal oxidation state associated to coordinated dative bonds than to that expected for covalent metal–ligand bonds. The metal charge varies continuously as the electronegativity of the donor atoms is varied, becoming close to the formal oxidation state when the ligands have a high electronegativity. The charge is less sensitive to changes in the metal oxidation state, a behavior that is in agreement with Pauling's electroneutrality rule. In general, thus, the oxidation state should be not considered as an approximation to the atomic charge, but as its upper limit, that is

approached as the ionicity of the metal–ligand bonds increases.

The formal oxidation states provide a framework for understanding and organizing chemical and physical properties of families of compounds. Complexes with a metal atom in the same oxidation state and different ligands may present quite different values of the calculated atomic charges, just a reflection of the varying degree of covalency of the metal–ligand bonds. From a chemical point of view, those compounds in the same oxidation state are formally related via ligand substitution processes, and present similar stereochemistries. Conversely, complexes with the same ligand set but in different oxidation states are related through redox (chemical or electrochemical) processes, the metal–ligand bond distances follow consistent trends, and so do the stereochemistry of the coordination sphere. An interesting outcome of the Pauling electroneutrality rule is that the population of the x^2–y^2 d orbital in complexes with not highly electronegative donor atoms is very similar in the Cu[II] and Cu[III] analogs. However, that population has a net spin in the former case, since it comes from both an unpaired electron and electron pair donation from the ligands. On the other hand, in the Cu[III] complexes, the electron population of x^2–y^2 has no net spin density, since it comes only from donation of electron pairs from the ligand.

Among the d^0 tetrahedral complexes analyzed, we find that the metal atomic charges are practically constant if the ligands are the same and the metal oxidation state is varied, e.g., in the series of oxoanions of V[V], Cr[VI] and Mn[VII], and much closer to zero than to the value of the oxidation state, in good qualitative agreement with the expectations of Pauling's electroneutrality rule. An additional argument against the use of the results of population analysis to discuss the oxidation state comes from the comparison of a d^0 and a d^5 ion. Both have the same population at the d orbitals (close to 5), but without a net spin density in the former case, as corresponds to partial donation of electron pairs from the ligands, and with a net spin density close to five in the latter case, as corresponds to unpaired electrons formally assigned to the metal atom. An interesting related study of the relationship between oxidation state and formal charges in solid state compounds has been published by Jansen and Wedig [20] after submission of this paper.

Appendix: Computational details

Unrestricted density functional calculations were carried out using the GAUSSIAN03 package [21], with the B3LYP hybrid method that employs the Becke three parameters exchange functional [22] and the Lee-Yang-Parr correlation functional [23]. An all-electron triple-ζ basis set was used for all transition metals [24], supplemented with two polarization functions [24, 25]. A basis set of similar quality was used for the main group elements [24], supplemented with extra polarization and diffuse functions, except for the H atoms not bonded to a metal [25]. An effective core pseudopotential was used for I [26] and Sb [27]. The following complexes were fully optimized: $[Cu^{III}L_4]^{3+}$ (L = He, NH_3, PH_3, AsH_3, SbH_3), $[Cu^{III}X_4]^-$ (X = H, CF_3, CH_3, SiH_3, SnH_3, F, Cl, Br, I, OH, SH and SeH), $[Cu^{II}L_4]^{2+}$ (L = He, NH_3 and PH_3), $[Cu^{II}X_4]^{2-}$ (X = H, CF_3 and Cl), $[Cu^{I}L_4]^+$ (L = He, NH_3 and PH_3), $[Cu^{I}X_4]^{3-}$ (X = H, CF_3), $[ScF_4]^-$, $[TiF_4]$, $[VF_4]^+$, $[VOF_3]$, $[CrO_2F_2]$, $[MnO_3F]$, $[VO_4]^{3-}$, $[CrO_4]^{2-}$ and $[MnO_4]^-$. The geometries of all Cu complexes were verified to correspond to minima in the potential energy surface through vibrational analyses. The $[Cu^{I}X_4]^{3-}$ anions (X = F, Cl, Br and I) have not been included in this study because they had been found previously to be unstable toward ligand dissociation [28]. The calculated charges reported were obtained from a natural population analysis [29], but the same qualitative trends were obtained with the atomic polar tensors (APT) method [30] (see Supporting Information).

References

1. Mingos DMP (1998) Essential trends in inorganic chemistry. Oxford University Press, Oxford
2. Jones CJ (2002) d- and f-Block chemistry. Wiley, New York
3. Pearson RG (2005) Chemical hardness. Wiley, Weinheim
4. Alvarez S, Hoffmann R, Mealli C (2008) (submitted)
5. Snyder JP (1995) Angew Chem Int Ed Engl 34:80. doi:10.1002/anie.199500801
6. Kaupp M, Schnering HGV (1995) Angew Chem Int Ed Engl 34:986
7. Snyder JP (1995) Angew Chem Int Ed Engl 34:986. doi:10.1002/anie.199509862
8. Pauling L (1948) J Chem Soc 1461. doi:10.1039/jr9480001461
9. Pauling L (1960) The nature of the chemical bond. Cornell University Press, Ithaca
10. Zanello P (2003) Inorganic electrochemistry. Theory, practice and application. Royal Society of Chemistry, Cambridge
11. Lever ABP (1990) Inorg Chem 29:1271. doi:10.1021/ic00331a030
12. Cirera J, Ruiz E, Alvarez S (2008) Inorg Chem 47:2871. doi:10.1021/ic702276k
13. Alvarez S, Alemany P, Casanova D, Cirera J, Llunell M, Avnir D (2005) Coord Chem Rev 249:1693. doi:10.1016/j.ccr.2005.03.031
14. Harwell DE, McMillan J, Knobler CB, Hawthorne MF (1997) Inorg Chem 36:5951. doi:10.1021/ic9706313
15. Eujen R, Hoge B, Brauer DJ (1996) J Organomet Chem 519:7. doi:10.1016/S0022-328X(96)06142-6
16. Naumann D, Roy T, Tebbe K-F, Crump W (1993) Angew Chem Int Ed Engl 32:1482. doi:10.1002/anie.199314821
17. Schlueter JA, Geiser U, Williams JM, Wang HH, Kwok W-K, Fendrich JA, Carlson KD, Achenbach CA, Dudek JD, Naumann D, Roy T, Schirber JE, Bayless WR (1994) J Chem Soc Chem Commun 1599
18. Jung D, Whangbo M-H, Alvarez S (1990) Inorg Chem 29:2252. doi:10.1021/ic00337a015
19. Lowe JP (1978) Quantum chemistry. Academic Press, London
20. Jansen M, Wedig U (2008) Angew Chem Int Ed 47:2. doi:10.1002/anie.200803605
21. Frisch MJ, Trucks GW, Schlegel HB, Scuseria GE, Robb MA, Cheeseman JR, Montgomery JA, Vreven T, Kudin KN, Burant JC, Millam JM, Iyengar SS, Tomasi J, Barone V, Mennucci B, Cossi M, Scalmani G, Rega N, Petersson GA, Nakatsuji H, Hada M, Ehara M, Toyota K, Fukuda R, Hasegawa J, Ishida T, Nakajima T, Honda Y, Kitao O, Nakai H, Klene M, Li X, Knox JE, Hratchian HP, Cross JB, Adamo C, Jaramillo J, Gomperts R, Stratmann RE, Yazyev O, Austin AJ, Cammi R, Pomelli C, Ochterski J, Ayala PY, Morokuma K, Voth GA, Salvador P, Dannenberg JJ, Zakrzewski VG, Dapprich S, Daniels AD, Strain MC, Farkas O, Malick DK, Rabuck AD, Raghavachari K, Foresman JB, Ortiz JV, Cui Q, Baboul AG, Clifford S, Cioslowski J, Stefanov BB, Liu G, Liashenko A, Piskorz P, Komaromi I, Martin RL, Fox DJ, Keith T, Al-Laham MA, Peng CY, Nanayakkara A, Challacombe M, Gill PMW, Johnson B, Chen W, Wong MW, Gonzalez C, Pople JA (2004) Gaussian Inc., Wallingford, CT
22. Becke AD (1993) J Chem Phys 98:5648. doi:10.1063/1.464913
23. Lee C, Yang W, Parr RG (1988) Phys Rev B 37:785. doi:10.1103/PhysRevB.37.785
24. Schäfer A, Huber C, Ahlrichs R (1994) J Chem Phys 100:5829. doi:10.1063/1.467146
25. Schäfer A, Horn H, Ahlrichs R (1992) J Chem Phys 97:2571. doi:10.1063/1.463096
26. Peterson KA, Figgen D, Goll E, Stoll H, Dolg M (2003) J Chem Phys 119:11113. doi:10.1063/1.1622924
27. Metz B, Stoll H, Dolg M (2000) J Chem Phys 113:2563. doi:10.1063/1.1305880
28. Carvajal MA, Alvarez S, Novoa JJ (2004) J Am Chem Soc 126:1465. doi:10.1021/ja038416a
29. Reed AE, Curtiss LA, Weinhold F (1988) Chem Rev 88:899. and references therein. doi:10.1021/cr00088a005
30. Cioslowski J (1989) J Am Chem Soc 111:8333. doi:10.1021/ja00204a001